Transformation of 2D Group-III Selenides to Ultra-thin Nitrides: Enabling Epitaxy on Amorphous Substrates

*Natalie Briggs, Maria Isolina Preciado, Yanfu Lu, Ke Wang, Jacob Leach, Xufan Li, Kai Xiao, Shruti Subramanian, Baoming Wang, Aman Haque, Susan Sinnott, Joshua A. Robinson**

N. Briggs, M. I. Preciado, S. Subramanian, Prof. J. A. Robinson
Department of Materials Science & Engineering, N-337 Millennium Science Complex, University Park PA, 16802, USA
Email: jar403@psu.edu

M. I. Preciado
Departamento de Ciencia de Materiales, E.T.S.I. Caminos, Canales y Puertos, Universidad Politecnica de Madrid, Madrid, E-28040, Spain

Y. Lu, Prof. S. Sinnott
Department of Materials Science & Engineering, Steidle Building, State College, PA, 16803, USA

Dr. K. Wang
Materials Characterization Laboratory, University Park, PA, 16802, USA

Dr. J. Leach
KYMA Technologies, 8829 Midway West Road, Raleigh, North Carolina 27617, USA

Dr. X. Li, Dr. K. Xiao
Center for Nanophase Materials Sciences, Oak Ridge National Laboratory, One Bethel Valley Road, Oak Ridge, Tennessee, 37831, USA

Dr. B. Wang, Prof. A. Haque
Department of Mechanical and Nuclear Engineering, The Pennsylvania State University, University Park, Pennsylvania 16802, USA

Keywords: 2D materials, nitrides, gallium selenide, ammonolysis, epitaxy

Abstract

The experimental realization of two-dimensional (2D) gallium nitride (GaN) has enabled the exploration of 2D nitride materials beyond boron nitride. Here we demonstrate one possible pathway to realizing ultra-thin nitride layers through a two-step process involving the synthesis of naturally layered, group-III chalcogenides (GIIIC) and subsequent annealing in ammonia (ammonolysis) that leads to an atomic-exchange of the chalcogen and nitrogen species in the 2D-GIIICs. The effect of nitridation differs for gallium and indium selenide, where gallium selenide undergoes structural changes and eventual formation of ultrathin GaN, while indium selenide layers are primarily etched rather than transformed by nitridation. Further investigation of the resulting GaN films indicates that ultra-thin GaN layers grown on silicon dioxide act as effective “seed layers” for the growth of 3D GaN on amorphous substrates.

Introduction

Significant advances in the field of two-dimensional (2D) materials for electronic applications have been made in recent years.[1,2] While research to date in the field of two-dimensional (2D) materials has largely focused on 2D transition metal dichalcogenides (TMDs) such as MoS_2 and WSe_2, 2D group-III chalcogenide (GIIIC) materials have also emerged as promising candidates for electronics.[3–5] Aside from the desirable properties of these materials such as high electron mobility (indium selenide (InSe)),[3] high photoresponsivity,[6,7] and large band gaps (gallium selenide and sulfide (GaSe, GaS)),[8] GIIICs may be used in ways that TMDs cannot: to realize ultra-thin and 2D nitrides. Group-III nitrides (gallium, indium, and aluminum nitride (GaN, InN, AlN), and their alloys) are commonly considered the most technologically relevant materials to emerge since silicon, acting as key materials in light emitting diodes, ultra-high frequency transistors, and many sensing technologies.[9,10] Furthermore, 2D allotropes of GaN can be experimentally realized, where quantum confinement and a previously unobserved atomic structure in the form of Ga_2N_3 leads to an increase in the band gap to 5 eV.[11] Since this discovery, synthesis of nanoscale and 2D nitride materials has been further pursued in an attempt to harness the high speed and high power capabilities of bulk nitrides combined with the increased and tunable band gaps of 2D nitrides.[12] Here we demonstrate that GIIIC materials such as GaSe can be thermally treated in ammonia (NH_3) to form ultra-thin GaN layers on amorphous silicon dioxide. Conversely, under similar conditions, InSe layers are merely etched during the nitridation process, indicating differences in atomic-level interactions and stability of the GIIIC materials. Furthermore, we demonstrate that ultrathin GaN layers provide a route for the realization of bulk GaN on SiO_2/Si substrates, opening the door for further investigation of III-V synthesis on amorphous substrates. The results of this work contrast studies which investigate bulk, exfoliated layers of GaSe that suggest bulk, single crystal GaN is possible via nitridation of GaSe.[13,14] We investigate the effects of these treatments further, through studies that examine synthesized, monolayer GaSe and the evolution of transformation to GaN as a function of GaSe thickness. While these studies investigate phase transformations of GIIIC materials in an NH_3 environment, they also serve to demonstrate ways in which 2D materials may be used beyond their intrinsic properties and chemistries, as stepping stones to the realization of new forms of materials and routes of synthesis.

Experimental

Few-layer GaSe is synthesized via powder vaporization of bulk GaSe crystals placed beneath face-down substrates. GaSe synthesis is carried out at 700°C - 850°C under a constant flow of 200 standard cubic centimeters per minute (sccm) argon (Ar) and a pressure of 300 Torr.[5] The bulk precursor is synthesized by combining gallium (Ga) metal (99.999%, Sigma Aldrich) with Ga_2Se_3 powder (99.99%, Alfa Aesar) in a 1:1 atomic ratio and heating this mixture in a sealed ampoule at 960ºC.[5] Substrates used in these studies include 300nm SiO_2/Si and epitaxial graphene grown via silicon sublimation from silicon carbide.[15] Following synthesis, GaSe layers are annealed in a 1:1 NH_3/Ar atmosphere at 600°C and 600 Torr for 30 minutes. Atomic force microscopy (AFM) measures surface roughness of the material before and after nitridation and scanning electron microscopy (SEM) allows for assessment of surface morphology. Transmission electron microscopy (TEM) and scanning transmission electron microscopy (STEM) provide information on atomic-scale crystallinity of the layers, while selected area electron diffraction (SAED) shows the crystal structure of the regions observed with STEM. Energy dispersive spectroscopy (EDS) provides elemental maps of the synthesized and nitridated materials. Density functional theory (DFT) calculations provide insight to the GaSe→GaN transformation, and are carried out using the Vienna Ab initio Simulation Package using the plane-wave basis and projector augmented wave method.[16,17] The Perdew-Burke-Ernzerhoff generalized gradient functional is chosen to be the exchange-correlational functional.[18] A 550 eV cutoff energy is used when the convergence tests indicate

that energies are converged to within 1 meV/atom with a 15x15x1 k-point mesh. Spin-polarization is applied in all the calculations and structure relaxation is iterated until energy differences are below 10^{-6} eV and until all forces on the atoms are below 0.05 eV/Å.

Results and Discussion

The synthesis of GaSe via powder vaporization (PV) leads to single crystal, micron-scale domains of mono- to few-layer GaSe on SiO_2 and graphene substrates. While as-grown GaSe layers may be investigated for their intrinsic properties, layers resulting from exposure to NH_3 environments provide a means to investigate the formation of nitride materials in a new context. Specifically, annealing GaSe layers in NH_3 between 600 – 700ºC leads to the formation of ultra-thin GaN layers. TEM and SAED of GaSe before and after nitridation verifies the transformation from GaSe to GaN (Figure 1a,b). However, rather than transforming to single crystal "2D" GaN, the nitridated GaSe forms a highly textured, ~0.8nm thick nanocrystalline wurtzite GaN layer (Figure 1a,b). Nanocrystalline material is also observed following ammonolysis of exfoliated GaSe layers through an increase in surface roughness (0.1nm to 0.5nm), further indicating a chemical reaction and structural modification has taken place. While this result contradicts previous reports,[13] the severe lattice mismatch between GaSe (3.755 Å)[19] and wurtzite GaN (3.189Å)[20] as well as different charge states of the Ga when bonded as GaSe versus GaN suggest that maintaining a single-crystal monolayer GaSe to GaN transformation throughout nitridation is unlikely without additional external stabilizing forces.

Nitridation of layered selenides is unique to the GIII element involved. To investigate the effect of NH_3 on different GIIICs, exfoliated InSe layers are also subject to ammonolysis at temperatures >500°C. Evident through optical microscopy, nitridation leads to an etching effect of the InSe layers, rather than the transformation of layers to InN (Supporting Information Figure S1 a,b). Furthermore, EDS of cross-sections of nitridated InSe layers demonstrates that the nitridation process is not an effective means of achieving conversion from InSe to InN at temperatures where the NH_3 is thermally decomposed. Instead, the majority of the layers remain composed of In and Se, with nitrogen (N) being nearly indistinguishable from the background signal, even with extended periods (>90 minutes) of NH_3 exposure (Figure S1 c – f). Despite the likely presence of some InN species, the effect of NH_3 atmospheres on InSe layers differs significantly from that of GaSe. It should be noted that even with the low efficiency of decomposition of NH_3 at nitridation temperatures, GaSe transforms to GaN, verifying that enough NH_3 decomposes during the nitridation processes to move GaSe conversion reactions forward. Thus, while the investigation of InSe to InN transformation is intriguing, it may require lower temperatures than currently possible in this study due to thermal limitations in cracking NH_3. One possible solution may be to utilize a plasma-enhanced nitridation process that could enable low-temperature studies with reactive nitrogen species.

The transformation of GaSe to GaN involves the structural decomposition of GaSe followed by reaction with nitrogen. This is evident when investigating thick, multilayer GaSe, which requires extended ammonolysis for complete transformation. Multilayer (~30 - 50nm) GaSe exposed to NH_3 for 30 minutes is not fully transformed, and instead exhibits a bilayer-type structure, where the top-most layers are transformed to $Ga_xSe_yN_z$ and the bottom layers remain single crystal GaSe (Figure 1 e,f). EDS maps of the partially nitridated GaSe (Figure 1g,h) qualitatively indicate Se deficiency in the outer, amorphous region, along with a small N signal (the bright sample outline in Figure 1g and h corresponds to false signal generated from the protective gold coating applied during sample preparation). Furthermore, XPS of GaSe as a function of nitridation time (Supporting Information Figure 2) shows a decrease in the Se 3d signal with increasing nitridation time, indicating a time dependence on the transformation of GaSe layers to GaN. X-ray photoelectron spectroscopy also shows consistent intensity of Ga 2p peaks for these

samples, indicating that no significant loss of Ga occurs during nitridation. Identification of the N 1s peak following ammonolysis is not possible due to a severe overlap with the Ga auger line shape near the expected energy of N 1s in GaN (397 eV).[21,22] This overlap is observed in samples even following the ammonolysis process, due to non-uniform GaSe thicknesses present following GaSe growth, and is evident from comparison of the Ga LMM-N 1s region for a number of reference samples including GaN, GaAs, SiN, and GaSe (Supporting Information Figure S3).To further understand the Ga LMM-N 1s line shape in nitridated samples, synthetic spectra are constructed using reference samples, where variation of the Ga:N ratio shows predicted spectra for different levels of N incorporation. These spectra indicate that reasonable observation of a N 1s peak in nitridated samples is unlikely when Ga:N is greater than 3:1 or 4:1 (Supporting Information Figure S4). Thus, while XPS can be used to observe changes in Se signal following ammonolysis, it cannot provide direct evidence of nitride formation, due to variation in grown GaSe thickness across the substrates. To further investigate the impact of GaSe thickness on nitridation, TEM studies are performed on mono- and multilayer GaSe samples.

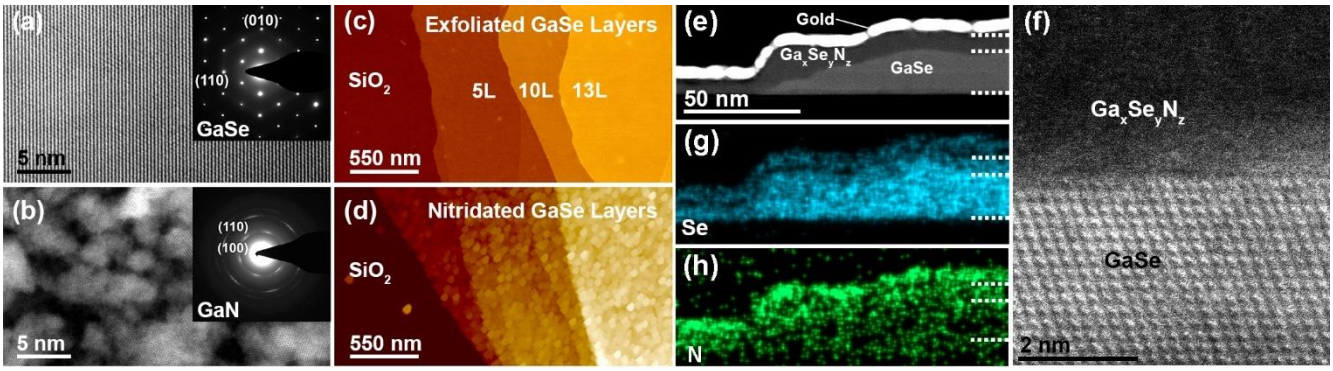

Figure 1. High resolution TEM images of GaSe before (a) and after (b) nitridation (where insets of (a) and (b) show the corresponding SAED patterns, confirming the starting GaSe and ending wurtzite GaN), and AFM images of exfoliated GaSe layers before (c) and after (d) nitridation. Image (e) shows a lower magnification cross-sectional STEM image of multilayer, nitridated GaSe. Magnification of the boundary between light and dark regions within the flake in (e) gives the STEM image (f), which shows an amorphous $Ga_xSe_yN_z$ outer region and crystalline GaSe inner region following nitridation. Images (g) and (h) show EDS maps of Se and N corresponding to the region shown in image (e). The top-most region of the EDS maps show signal from the heavy, protective gold coating. A slight decrease in Se can be observed in the outer regions of the cross-section (g) and a slight N signal can be seen in this region as well (h).

The presence of an amorphous, ternary outer layer in partially transformed bulk GaSe (shown in Figure 1f) suggests that rather than a simple Se and N exchange, transformation to GaN requires significant structural modifications. At roughly 600°C, Se loss occurs due to thermal decomposition of GaSe, which likely leads to Ga dangling bonds, and enables nitridation of the GaSe structure.[5] Density functional theory (DFT) calculations are performed to quantify the energetic information associated with initial, potential intermediate, and final structures.[16] The reaction investigated is $GaSe + NH_3 \rightarrow GaN + Se + \frac{3}{2}H_2$, which considers that ammonia decomposes into atomic nitrogen and amine fragments at elevated temperatures. Specifically, DFT analysis is used to investigate the introduction of N into bulk GaSe as well as the removal of Se from bulk GaN, where N, NH_x, and Se atoms are in gaseous form. It should be noted that analysis includes the addition of atomic energies of Se and N in their most stable forms to the total energy of the reaction in order to balance the total number of each type of atom involved.

Density functional theory results indicate that bulk GaN is more stable than bulk GaSe, where the difference in the energy of formation between the two materials is 2.306 eV/atom (Figure 2). To further investigate the transformation process, two mechanisms are considered: 1) the occupation of interstitial sites in GaSe by N atoms which can subsequently fill the space of Se atoms that leave the GaSe surface, and 2) the formation of Se vacancies on the surface of bulk GaSe followed by occupation of these vacancies with N atoms. Calculations reveal that the energy barrier for N atoms transitioning from absorption on the GaSe surface to occupation of an interstitial site in bulk GaSe is +0.096 eV/atom (Figure 2b), and that the movement of atomic N from an interstitial site to a Se vacancy requires an additional +0.071 eV/atom (N_{hop} in Figure 2). This value is relatively small compared to the +0.625 eV/atom associated with N directly substituting a Se vacancy (Figure 2c). For comparison, the energy barrier to achieving substitutional and interstitial Se are 0.042 eV/atom and 0.051 eV/atom in bulk GaN, respectively (displayed relative to GaN in Figure 2d). Consequently, the case of Se leaving bulk GaN is predicted to take place via departure from a substitutional site and from an interstitial site.

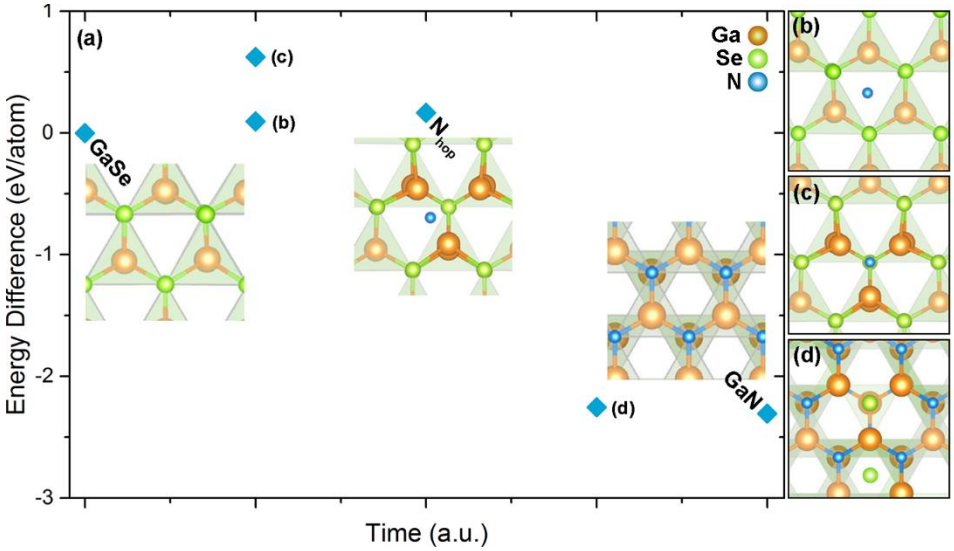

Figure 2. Formation energies with respect to bulk GaSe are shown in (a) and atomistic configurations in (b-d). (b) corresponds to a N interstitial in bulk GaSe, (c) corresponds to N substitution in bulk GaSe, and (d) corresponds to both a Se interstitial and substitution in bulk GaN, where both configurations are displayed in the image and a single point represents the associated energies, which fall within 0.01eV/atom of each other. The energy barrier of an N atom hopping from an interstitial in GaSe to a Se vacancy is shown by N_{hop}. The possible reaction route follows (b)→N_{hop}→(d).

While nanocrystalline in nature, the formation of ultra-thin, GaN layers from GaSe holds particular promise in the context of "seed layers" for the synthesis of thick GaN on amorphous substrates. Typically, crystalline GaN films require crystalline substrates such as sapphire and silicon carbide rather than amorphous substrates.[23] However, van der Waals materials like GaSe may be grown on a wide range of substrates, both crystalline and amorphous.[5,24] Thus, utilizing GaSe as a starting material offers the potential to realize GaN on amorphous substrates such as silica (SiO_2). To test this hypothesis, mono- to few-layer GaSe is grown on 300nm SiO_2/Si substrates via PV at 700°C (Supporting Information Figure S5). These layers are then nitridated at 600°C and 600 Torr for 30 minutes, resulting in ultrathin, polycrystalline GaN such as that shown in Figure 1b. Subsequently, GaN films with thicknesses of roughly 850nm are grown on the transformed 2D layers via hydride vapor phase epitaxy (HVPE). GaN

films are grown in a vertical HVPE reactor at 1030°C using gallium chloride and NH_3 for the group III and group V precursors, respectively. The recipe scheme is similar to processes typically utilized to produce undoped thin films of GaN on AlN on Si.[25,26] Interestingly, GaN growth on regions without a seed layer (e.g. bare SiO_2) is precluded, while regions where GaN films exist differ dramatically based on the initial layer thickness of the nitridated GaSe (Figure 3). GaN films grown on monolayer seed regions (Fig. 3a) exhibit a rough surface morphology and appear polycrystalline in nature, while GaN films grown on transformed few-layer GaSe exhibit smooth surfaces and maintain the triangular morphology of the starting GaSe (Fig. 3b). In regions where the GaSe exhibits a mono- to few-layers, a transformation from polycrystalline to single crystalline GaN is directly observed (Fig. 3c). This is verified using selected area electron diffraction (SAED) of the two distinct regions (Fig. 3c, insets), where GaN films grown on few-layer seeds are single-crystal in nature, while monolayer seeds lead to polycrystalline GaN films. SAED patterns in Figure 3 correspond to acquisition locations 200nm above the GaN/SiO_2 interface. In addition to impacting the microstructure, cross-sectional scanning transmission electron microscopy (STEM) (Fig. 3c-f) indicates that there are also fewer defects at the SiO_2/GaN interface in the case of GaN grown on thicker seed layers. There may be several reasons for this phenomenon to occur. The first possibility is that the transformation of GaSe→GaN leads to significant structural changes that result in nano-sized holes in monolayer GaN films (Fig. 1b), which in turn exposes the HVPE-grown GaN to bare SiO_2. This subsequently interrupts the epitaxy process (GaN does not grow directly on SiO_2), thereby leading to polycrystalline, rough films due to the heterogeneous surface. Alternatively, or additionally, thicker few-layer seeds are able to screen the effects of the amorphous substrate, while monolayers are not. Such a phenomenon would be similar to recent reports of graphene acting as a transparent release layer for semiconductor epitaxy.[27]

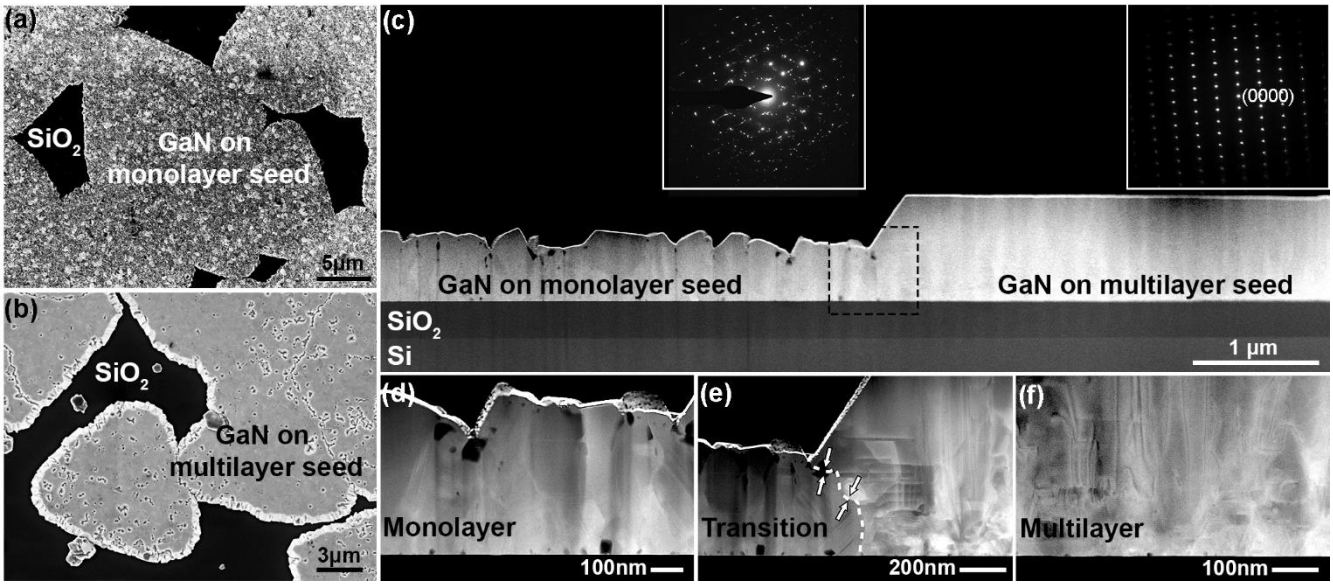

Figure 3: Scanning electron microscopy (a, b) and cross-sectional STEM (c-f) images show GaN films grown on transformed GaSe seed layers, where thinner seed layers (monolayer) result in rougher GaN surfaces (a, c, d), and thicker seed layers (few-layer) result in smoother GaN formation (b, c, f). (c-f) show cross-sectional STEM images of the two regions, where GaN films on monolayer seed regions show greater defects and surface roughness (c, d, e). Corresponding SAED patterns in (c) are shown for both film types, acquired at locations 200nm above the GaN/SiO_2 interface. of High magnification STEM images of GaN on mono- and few-layer seeds are shown in (d) and (f). (e) shows a region of transition from GaN grown on monolayer to GaN grown on few-layer seeds (also outlined with the dotted box in (c)). The dotted line in (e) outlines a hypothesized boundary between GaN grown on mono- and few-layer seeds.

Conclusions

This study reveals that group-III selenide to nitride formation leads to massive structural transformations resulting in either amorphization and recrystallization (GaSe→GaN) or etching/vaporization of the layers (InSe). In the case of GaSe, the transformation leads to nanocrystalline GaN layers. While one may suggest this process leads to merely "low-quality" ultra-thin GaN films, these ultrathin layers act as excellent seeds for synthesis of thick GaN films on amorphous substrates. Interestingly, the morphology and crystallinity of the resulting GaN films is dictated by the seed layer thickness, where few-layer seeds yield single-crystal GaN overlayers and monolayer seeds yield polycrystalline films. Utilization of such seed layers could enable high quality GaN synthesis on amorphous substrates such as silica and glass, thereby expanding the functionality of nitride materials and the library of possible growth substrates.

Acknowledgements

This research was supported by the Army Research Office (Grant # W911NF1510488) and the 2D Crystal Consortium NSF Materials Innovation Platform under cooperative agreement DMR-1539916. JAR and SS acknowledge NSF support through the CAREER Grant 1453924. Synthesis of the GaSe precursor and some mono/few-layer GaSe was conducted at the Center for Nanophase Materials Sciences, which is a DOE Office of Science User Facility. Special thanks to Jeffrey R. Shallenberger and the Penn State Materials Characterization Laboratory for contributing synthetic x-ray photoelectron spectra.

References

[1] T. Kim, J. Mun, H. Park, D. Joung, M. Diware, C. Won, J. Park, S.-H. Jeong, S.-W. Kang, *Nanotechnology* **2017**, *28*, 18LT01.

[2] J. S. Ross, P. Klement, A. M. Jones, N. J. Ghimire, J. Yan, D. G. Mandrus, T. Taniguchi, K. Watanabe, K. Kitamura, W. Yao, D. H. Cobden, X. Xu, *Nat. Nanotechnol.* **2014**, *9*, 268.

[3] D. A. Bandurin, A. V Tyurnina, G. L. Yu, A. Mishchenko, V. Zólyomi, S. V Morozov, R. K. Kumar, R. V Gorbachev, Z. R. Kudrynskyi, S. Pezzini, Z. D. Kovalyuk, U. Zeitler, K. S. Novoselov, A. Patanè, L. Eaves, I. V Grigorieva, V. I. Fal, A. K. Geim, Y. Cao, *Nat. Nanotechnol.* **2016**, 1.

[4] P. Hu, Z. Wen, L. Wang, P. Tan, K. Xiao, *ACS Nano* **2012**, *6*, 5988.

[5] X. Li, M.-W. Lin, A. Puretzky, J. C. Idrobo, C. Ma, M. Chi, M. Yoon, C. M. Rouleau, I. I. Kravchenko, D. B. Geohegan, K. Xiao, *Sci. Rep.* **2014**, *4*, 5497.

[6] S. Lei, L. Ge, Z. Liu, S. Najmaei, G. Shi, G. You, J. Lou, R. Vajtai, P. M. Ajayan, *Nano Lett.* **2013**, *13*, 2777.

[7] G. W. Mudd, S. A. Svatek, L. Hague, O. Makarovsky, Z. R. Kudrynskyi, C. J. Mellor, P. H. Beton, L. Eaves, K. S. Novoselov, Z. D. Kovalyuk, E. E. Vdovin, A. J. Marsden, N. R. Wilson, A. Patanè, *Adv. Mater.* **2015**, *27*, 3760.

[8] C. S. Jung, F. Shojaei, K. Park, J. Y. Oh, H. S. Im, D. M. Jang, J. Park, H. S. Kang, *ACS Nano* **2015**, *9*, 9585.

[9] O. Ambacher, *J. Phys. D. Appl. Phys.* **1998**, *31*, 2653.

[10] M. Asif Khan, M. Shatalov, H. P. Maruska, H. M. Wang, E. Kuokstis, *Jpn. J. Appl. Phys.* **2005**, *44*, 7191.

[11] Z. Y. Al Balushi, K. Wang, R. K. Ghosh, R. A. Vila, S. M. Eichfeld, J. D. Caldwell, X. Qin, Y.-C. Lin, P. A. DeSario, G. Stone, S. Subramanian, D. F. Paul, R. M. Wallace, S. Datta, J. M. Redwing, J. A. Robinson, *Nat Mater* **2016**, *15*, 1166.

[12] B. Liu, W. Yang, J. Li, X. Zhang, P. Niu, X. Jiang, *Nano Lett.* **2017**, *17*, 3195.

[13] M. B. Sreedhara, K. Vasu, C. N. R. Rao, *Zeitschrift Fur Anorg. Und Allg. Chemie* **2014**, *640*, 2737.

[14] U. K. Gautam, S. R. C. Vivekchand, A. Govindaraj, C. N. R. Rao, *R. Soc. Chem.* **2005**, 3995.

[15] C. Riedl, C. Coletti, U. Starke, *J. Phys. D. Appl. Phys.* **2010**, *43*, 1.

[16] P. E. Blöchl, *Phys. Rev. B* **1994**, *50*, 17953.

[17] G. Kresse, J. Furthmu, *Phys. Rev. B* **1996**, *54*, 11169.

[18] J. P. Perdew, K. Burke, M. Ernzerhof, *Phys. Rev. Lett.* **1996**, *77*, 3865.

[19] A. Kuhn, A. Chevy, R. Chevalier, *Phys. status solidi* **1975**, *31*, 469.

[20] M. Leszczynski, H. Teisseyre, T. Suski, I. Grzegory, M. Bockowski, J. Jun, S. Porowski, K. Pakula, J. M. Baranowski, C. T. Foxon, T. S. Cheng, *Appl* **1996**, *69*, 73.

[21] J. Carin, R, Deville, J. P., Werckmann, *Surf. Interface Anal.* **1990**, *16*, 65.

[22] J. Hedman, N. Martensson, *Phys. Scr.* **1980**, *22*, 176.

[23] T. Paskova, D. A. Hanser, K. R. Evans, *Proc. IEEE* **2010**, *98*, 1324.

[24] D. Ruzmetov, K. Zhang, G. Stan, B. Kalanyan, G. R. Bhimanapati, S. M. Eichfeld, R. A. Burke, P. B. Shah, T. P. O. Regan, F. J. Crowne, A. G. Birdwell, J. A. Robinson, A. V Davydov, T. G. Ivanov, *ACS Nano* **2016**, *10*, 3580.

[25] Y. Honda, M. Okano, M. Yamaguchi, N. Sawaki, *Phys. Status Solidi C Conf.* **2005**, *2*, 2125.

[26] A. Usui, H. Sunakawa, A. Sakai, A. Y. Atsushi, *Jpn. J. Appl. Phys.* **1997**, *36*, L899.

[27] Y. Kim, S. S. Cruz, K. Lee, B. O. Alawode, C. Choi, Y. Song, J. M. Johnson, C. Heidelberger, W. Kong, S. Choi, K. Qiao, I. Almansouri, E. A. Fitzgerald, J. Kong, A. M. Kolpak, J. Hwang, J. Kim, *Nat. Publ. Gr.* **2017**, *544*, 340.